

Analytic solutions for two and three dimensional flows of Maxwell fluid

by

Khansa Rubab Malik



A Dissertation submitted in partial fulfillment of the requirements
for the degree of Master of Philosophy in Mathematics

Supervised by

Dr. Meraj Mustafa Hashmi

School of Natural Sciences

National University of Sciences and Technology

Islamabad, Pakistan

© Khansa Rubab Malik, 2016

National University of Sciences & Technology

M.Phil THESIS WORK


We hereby recommend that the dissertation prepared under our supervision by: KHANSA RUBAB MALIK, Regn No. NUST201361967MSNS78013F Titled: Analytic Solutions for Two and Three Dimensional Flows of Maxwell Fluid be accepted in partial fulfillment of the requirements for the award of **M.Phil** degree.

Examination Committee Members

1. Name: DR. MUJEEB UR REHMAN

Signature: 

2. Name: DR. YOUSAF HABIB

Signature: 

3. Name: _____

Signature: _____

4. Name: DR. MASOOD KHAN

Signature: 

Supervisor's Name: MERAJ MUSTAFA HASHMI

Signature: 


Head of Department

09-09-2016
Date

COUNTERSIGNED

Date: 09/09/2016


Dean/Principal

This Dissertation is dedicated to

my loving Parents

for their endless love,

prayers and support

Acknowledgement

All the appreciations and praises are for the most omnipotent ALMIGHTY ALLAH, the lord of the world, the most Generous and Merciful that knows the hidden truth of this universe and the Holy Prophet Muhammad (PBUH) who declared “it is an obligatory duty of every Muslim to seek and acquire knowledge”.

First and foremost I would like to express my sincerest gratitude and deep regards to my supervisor Dr. Meraj Mustafa Hashmi, for providing precious time, encouragement and guidance. I am extremely grateful to him for his constant support throughout my research phase with his patience and knowledge which enabled me to complete my thesis work.

I would like to thank the GEC members Dr. Mujeeb ur Rehman and Dr. Yousaf Habib for their kind attitude and support. I also extend my gratitude to National University of Sciences and Technology (NUST) Islamabad, Pakistan, all faculty members at School of Natural Sciences (SNS) for supporting my research work.

I owe my heartiest thanks to my loving parents for their love, support and prayers throughout my life. Grandmother deserves to be especially mentioned, whose prayers have accompanied me through thick and thin. I would also like to thank my sister Warda for being caring and supportive.

A very special thanks to my dear friends Mehar Rasool, Anum Khaliq, Nadia Qamar, Shaista Kanwal and Memoona Qamar for their care, support and time.

Lastly, It is my pleasure to convey my gratitude to all my roomie friends including Azka Hassan, Hafsah Ashraf, Neelam Iqbal, Sidra Zia and Raheela Malik for their suggestions and cheerful companionship.

Khansa Rubab Malik

Preface

Boundary layer flow induced by the motion of stretching surfaces have special significance in numerous engineering and industrial processes. The processes of metal extrusion, manufacture of plastics and rubber, drawing of plastic film, wire drawing, food processing, glass fiber and paper production involve such flows. In such process, the quality of final product depends on the rate of cooling which is determined through the structure of thermal boundary layer near the moving sheet. This thesis deals with the analytic solutions of non-linear problems arising in the flow with heat/mass transfer of viscoelastic fluids over a stretching sheet. Constitutive equations for upper-convected Maxwell (UCM) fluid are taken into account. The energy equation through more general Cattaneo-Christov heat flux model is analyzed.

Chapter 1 is introductory and contains some basic definitions and concepts. Boundary layer equations governing the three dimensional flow and heat transfer of an upper-convected Maxwell fluid are also derived. A detailed review about the problem considered in subsequent chapters is presented. At the end, basic idea of homotopy analysis method (HAM) is explained.

Chapter 2 deals with the stagnation-point flow and mass transfer of Maxwell fluid. Here analytic solutions of the arising non-linear problem are constructed by HAM. Graphical results showing the influence of physical parameters on velocity and concentration fields are presented.

Chapter 3 is concerned with the magnetohydrodynamic (MHD) three-dimensional flow of upper-convected Maxwell (UCM) fluid over a bi-directional stretching surface by using the Cattaneo-Christov heat flux model. This model has tendency to capture the characteristics of thermal relaxation time. The governing partial differential equations even after employing the boundary layer approximations are

non linear. Accurate analytic solutions for velocity and temperature distributions are developed through well-known homotopy analysis method (HAM). It is noticed that velocity decreases and temperature rises when stronger magnetic field strength is accounted. Penetration depth of temperature is a decreasing function of thermal relaxation time. The analysis for classical Fourier heat conduction law can be obtained as a special case of the present work.

In chapter 4, the main conclusions of the thesis are reported .

Contents

1	Introduction	1
1.1	Newtonian fluids	1
1.2	Non-Newtonian fluids	1
1.2.1	Time independent fluids	2
1.2.2	Time dependent fluids	3
1.2.3	Viscoelastic fluids	3
1.3	Boundary layer equations for flow of an upper-convected Maxwell (UCM) fluid	4
1.4	Energy equation for three-dimensional flow through Cattaneo-Christov heat flux model	6
1.5	Homotopy Analysis Method (HAM)	7
1.5.1	Background	7
1.5.2	Basic idea of HAM	7
1.6	Literature survey	9
2	Stagnation point flow of an upper-convected Maxwell (UCM) fluid with mass transfer	12
2.1	Problem formulation	12
2.2	Series solutions	14
2.3	Convergence of homotopy solutions	17

2.4	Results and discussion	19
3	MHD three-dimensional flow of upper-convected Maxwell fluid using Cattaneo-Christov heat flux model	23
3.1	Problem formulation	23
3.2	Analytic solutions by homotopy analysis method	26
3.3	Convergence of homotopy series solutions	30
3.4	Results and discussion	31
4	Conclusions	37
	Bibliography	38

Chapter 1

Introduction

Fluids can be characterized as Newtonian and non-Newtonian based on their rheological behavior.

1.1 Newtonian fluids

Newtonian fluids are distinguished by Newton's law of viscosity which states that shear stress is directly as well as linearly proportional to the deformation rate. Mathematically,

$$\tau_{yx} = \mu \frac{du}{dy}, \quad (1.1)$$

where μ is the dynamic viscosity, du/dy is the rate of strain and τ_{yx} denotes the shear stress. Most common Newtonian fluids are air, water, gasoline and organic solvents.

1.2 Non-Newtonian fluids

In contrast to the Newtonian-fluids, these fluids have non-linear relationship between stress and deformation rate. For such fluids, the power-law model holds.

Mathematically, for unidirectional flow the power-law model is given by

$$\tau_{yx} = K\left(\frac{du}{dy}\right)^n, \quad (1.2)$$

$$= \eta \frac{du}{dy}, \quad (1.3)$$

where $\eta = K(du/dy)^{n-1}$ is the apparent viscosity, n is the flow behavior index and K is the consistency index. Most common fluids under this category are pastes, ketchup, blood and polymer solutions. Non-Newtonian fluids are divided into three groups.

- Time independent fluids.
- Time dependent fluids.
- Viscoelastic fluids.

1.2.1 Time independent fluids

Apparent viscosity of such type of fluids is independent of the time for which stress is applied. These are further subdivided into three classes.

(a) Pseudoplastics ($\eta < 1$)

In these fluids, the apparent viscosity decreases with an increase in the deformation rate. These are also called shear thinning fluids. Examples includes cement, clay, syrup, blood, colloidal suspensions and polymer solutions.

(b) Dilatants ($\eta > 1$)

Dilatants are called shear thickening fluids, i.e their apparent viscosity increases with an increase in deformation rate. Examples includes quicksand and suspension of corn starch in water. Practically very few fluids behave in this manner.

(c) **Plastics**

Fluids which behave as a solid until a minimum yield stress τ_{yx} is exceeded and subsequently exhibits a linear relation between stress and rate of strain. Mathematically,

$$\tau_{yx} = A + B \left(\frac{du}{dy} \right)^n, \quad (1.4)$$

where A , B and n are constants. If $n = 1$, Eq. (1.4) represents Bingham plastic fluids. Examples of such fluids are jellies, drilling mud, clay suspension and sewage sludge.

1.2.2 **Time dependent fluids**

In this subclass of non-Newtonian fluids, apparent viscosity is dependent upon time. These fluids are further subdivided into two classes.

(a) **Thixotropic fluids**

Under the influence of constant applied shear stress, these fluids show a decrease in dynamic viscosity with time. Examples of such fluids are honey and thixotropic jelly paints.

(b) **Rheopectic fluids**

Under the influence of applied shear stress, these fluids show an increase in dynamic viscosity with time. Examples of such fluids include gypsum, pastes and suspension in water.

1.2.3 **Viscoelastic fluids**

Viscoelastic fluids possess both viscous and elastic properties. These fluids return back to their original shape when the stress is released.

Examples of viscoelastic materials would be toothpaste, gelatine and blood clots.

1.3 Boundary layer equations for flow of an upper-convected Maxwell (UCM) fluid

The constitutive equation for Maxwell fluid is

$$\rho \frac{d\mathbf{V}}{dt} = -\nabla p + \nabla \cdot \mathbf{S}, \quad (1.5)$$

$$\mathbf{S} + \lambda_1 \frac{D\mathbf{S}}{Dt} = \mu \mathbf{A}_1, \quad (1.6)$$

where $\mathbf{V} = [u(x, y, z), v(x, y, z), w(x, y, z)]$ is the velocity vector for three dimensional flow, \mathbf{S} is the extra stress tensor, μ is the dynamic viscosity, λ_1 is the fluid relaxation time, D/Dt is the convected time derivative and \mathbf{A}_1 is the first Rivlin-Erickson tensor defined as

$$\begin{aligned} \mathbf{A}_1 &= \nabla \mathbf{V} + (\nabla \mathbf{V})^t, \\ &= \begin{bmatrix} 2\frac{\partial u}{\partial x} & \frac{\partial u}{\partial y} + \frac{\partial v}{\partial x} & \frac{\partial u}{\partial z} + \frac{\partial w}{\partial x} \\ \frac{\partial u}{\partial y} + \frac{\partial v}{\partial x} & 2\frac{\partial v}{\partial y} & \frac{\partial v}{\partial z} + \frac{\partial w}{\partial y} \\ \frac{\partial u}{\partial x} + \frac{\partial w}{\partial z} & \frac{\partial v}{\partial x} + \frac{\partial w}{\partial z} & 2\frac{\partial w}{\partial z} \end{bmatrix}. \end{aligned} \quad (1.7)$$

For any vector $(\alpha)_i$, the convected time derivative D/Dt is given by

$$\frac{D}{Dt}(\alpha)_i = \frac{\partial}{\partial t}(\alpha)_i + \mathbf{V}_r(\alpha)_{i,r} - \mathbf{V}_{i,r}(\alpha)_r. \quad (1.8)$$

Assigning the operator $(1 + \lambda_1 \frac{D}{Dt})$ on both sides of Eq. (1.5), one obtains

$$\rho \left(1 + \lambda_1 \frac{D}{Dt}\right) \frac{d\mathbf{V}}{dt} = - \left(1 + \lambda_1 \frac{D}{Dt}\right) \nabla p + \left(1 + \lambda_1 \frac{D}{Dt}\right) (\nabla \cdot \mathbf{S}), \quad (1.9)$$

where

$$\frac{D}{Dt}(\nabla \cdot) = \nabla \cdot \left(\frac{D}{Dt}\right) \quad (1.10)$$

Taking into account Eq. (1.10) in Eq. (1.9) and then using Eq. (1.6), we arrive at the following:

$$\rho \left(1 + \lambda_1 \frac{D}{Dt} \right) \frac{d\mathbf{V}}{dt} = - \left(1 + \lambda_1 \frac{D}{Dt} \right) \nabla p + \nabla \cdot \left(1 + \lambda_1 \frac{D}{Dt} \right) \mathbf{S}, \quad (1.11)$$

$$= - \left(1 + \lambda_1 \frac{D}{Dt} \right) \nabla p + \mu (\nabla \cdot \mathbf{A}_1). \quad (1.12)$$

In the absence of pressure gradient, Eq. (1.12) takes the following form:

$$\rho \left(1 + \lambda_1 \frac{D}{Dt} \right) \frac{d\mathbf{V}}{dt} = \mu (\nabla \cdot \mathbf{A}_1). \quad (1.13)$$

The components of Eq. (1.13) are as under

$$\begin{aligned} \frac{\partial u}{\partial t} + u \frac{\partial u}{\partial x} + v \frac{\partial u}{\partial y} + w \frac{\partial u}{\partial z} &= \nu \left(\frac{\partial^2 u}{\partial x^2} + \frac{\partial^2 u}{\partial y^2} + \frac{\partial^2 u}{\partial z^2} \right) - \lambda_1 \left(\frac{\partial^2 u}{\partial t^2} + 2u \frac{\partial^2 u}{\partial x \partial t} + 2v \frac{\partial^2 u}{\partial y \partial t} \right. \\ &\quad + 2w \frac{\partial^2 u}{\partial z \partial t} + u^2 \frac{\partial^2 u}{\partial x^2} + v^2 \frac{\partial^2 u}{\partial y^2} + w^2 \frac{\partial^2 u}{\partial z^2} + 2uv \frac{\partial^2 u}{\partial x \partial y} \\ &\quad \left. + 2vw \frac{\partial^2 u}{\partial y \partial z} + 2uw \frac{\partial^2 u}{\partial x \partial z} \right), \end{aligned} \quad (1.14)$$

$$\begin{aligned} \frac{\partial v}{\partial t} + u \frac{\partial v}{\partial x} + v \frac{\partial v}{\partial y} + w \frac{\partial v}{\partial z} &= \nu \left(\frac{\partial^2 v}{\partial x^2} + \frac{\partial^2 v}{\partial y^2} + \frac{\partial^2 v}{\partial z^2} \right) - \lambda_1 \left(\frac{\partial^2 v}{\partial t^2} + 2u \frac{\partial^2 v}{\partial x \partial t} + 2v \frac{\partial^2 v}{\partial y \partial t} \right. \\ &\quad + 2w \frac{\partial^2 v}{\partial z \partial t} + u^2 \frac{\partial^2 v}{\partial x^2} + v^2 \frac{\partial^2 v}{\partial y^2} + w^2 \frac{\partial^2 v}{\partial z^2} + 2uv \frac{\partial^2 v}{\partial x \partial y} + \\ &\quad \left. 2vw \frac{\partial^2 v}{\partial y \partial z} + 2uw \frac{\partial^2 v}{\partial x \partial z} \right). \end{aligned} \quad (1.15)$$

Utilizing the usual boundary layer approximations, Eq. (1.14) and Eq. (1.15) reduces to

$$\begin{aligned} u \frac{\partial u}{\partial x} + v \frac{\partial u}{\partial y} + w \frac{\partial u}{\partial z} &= \nu \frac{\partial^2 u}{\partial z^2} - \lambda_1 \left(u^2 \frac{\partial^2 u}{\partial x^2} + v^2 \frac{\partial^2 u}{\partial y^2} + w^2 \frac{\partial^2 u}{\partial z^2} + 2uv \frac{\partial^2 u}{\partial x \partial y} \right. \\ &\quad \left. + 2vw \frac{\partial^2 u}{\partial y \partial z} + 2uw \frac{\partial^2 u}{\partial x \partial z} \right), \end{aligned} \quad (1.16)$$

$$\begin{aligned} u \frac{\partial v}{\partial x} + v \frac{\partial v}{\partial y} + w \frac{\partial v}{\partial z} &= \nu \frac{\partial^2 v}{\partial z^2} - \lambda_1 \left(u^2 \frac{\partial^2 v}{\partial x^2} + v^2 \frac{\partial^2 v}{\partial y^2} + w^2 \frac{\partial^2 v}{\partial z^2} + 2uv \frac{\partial^2 v}{\partial x \partial y} \right. \\ &\quad \left. + 2vw \frac{\partial^2 v}{\partial y \partial z} + 2uw \frac{\partial^2 v}{\partial x \partial z} \right). \end{aligned} \quad (1.17)$$

1.4 Energy equation for three-dimensional flow through Cattaneo-Christov heat flux model

The energy equation in absence of viscous dissipation and heat generation/absorption is expressed as

$$\rho c_p (\mathbf{V} \cdot \nabla) T = -\nabla \cdot \mathbf{q}, \quad (1.18)$$

where ρ is the fluid density, c_p is the specific heat, $\mathbf{V} = [u(x, y, z), v(x, y, z), w(x, y, z)]$ is the velocity vector and \mathbf{q} is the heat flux. According to Christov [3], \mathbf{q} satisfies the following:

$$\mathbf{q} + \lambda_2 \left[\frac{\partial \mathbf{q}}{\partial t} + \mathbf{V} \cdot \nabla \mathbf{q} - \mathbf{q} \cdot \nabla \mathbf{V} + (\nabla \cdot \mathbf{V}) \mathbf{q} \right] = -k \nabla T, \quad (1.19)$$

in which λ_2 is the thermal relaxation time, k is the thermal conductivity of the fluid and T is the temperature of the Maxwell fluid. When $\lambda_2 = 0$, Eq. (1.19) reduces to the Fourier's law. For incompressible flow, $\nabla \cdot \mathbf{V} = 0$, and Eq. (1.19) becomes

$$\mathbf{q} + \lambda_2 \left[\frac{\partial \mathbf{q}}{\partial t} + \mathbf{V} \cdot \nabla \mathbf{q} - \mathbf{q} \cdot \nabla \mathbf{V} \right] = -k \nabla T. \quad (1.20)$$

Now we apply Del operator on Eq. (1.20)

$$\nabla \cdot \mathbf{q} + \lambda_2 \nabla \cdot \left[\frac{\partial \mathbf{q}}{\partial t} + \mathbf{V} \cdot \nabla \mathbf{q} - \mathbf{q} \cdot \nabla \mathbf{V} \right] = -\nabla \cdot (k \nabla T). \quad (1.21)$$

Make use of the following identities

$$\frac{\partial}{\partial t} (\nabla \cdot) = \nabla \cdot \left(\frac{\partial}{\partial t} \right) \quad (1.22)$$

$$\nabla \cdot (\mathbf{V} \cdot \nabla \mathbf{q}) = \mathbf{V} \cdot \nabla (\nabla \cdot \mathbf{q}) + \nabla \mathbf{V}; \nabla \mathbf{q} \quad (1.23)$$

$$\nabla \cdot (\mathbf{q} \cdot \nabla \mathbf{V}) = \mathbf{q} \cdot \nabla (\nabla \cdot \mathbf{V}) + \nabla \mathbf{q}; \nabla \mathbf{V} \quad (1.24)$$

Eq. (1.21) takes the following form

$$-\nabla \cdot \mathbf{q} = \lambda_2 [(\nabla \cdot \mathbf{q})_t + \mathbf{V} \cdot \nabla (\nabla \cdot \mathbf{q})] + \nabla \cdot (k \nabla T) \quad (1.25)$$

In view of the above equation, Eq. (1.18) takes the following form

$$\rho c_p(\mathbf{V} \cdot \nabla)T = \lambda_2[(\nabla \cdot \mathbf{q})_t + \mathbf{V} \cdot \nabla(\nabla \cdot \mathbf{q})] + \nabla \cdot (k \nabla T), \quad (1.26)$$

Eq. (1.26) in component form is given below:

$$\begin{aligned} u \frac{\partial T}{\partial x} + v \frac{\partial T}{\partial y} + w \frac{\partial T}{\partial z} &= \frac{k}{\rho c_p} \frac{\partial^2 T}{\partial z^2} - \lambda_2 \left[u^2 \frac{\partial^2 T}{\partial x^2} + v^2 \frac{\partial^2 T}{\partial y^2} + w^2 \frac{\partial^2 T}{\partial z^2} + 2uv \frac{\partial^2 T}{\partial x \partial y} \right. \\ &\quad + 2vw \frac{\partial^2 T}{\partial y \partial z} + 2uw \frac{\partial^2 T}{\partial x \partial z} + \left(u \frac{\partial u}{\partial x} + v \frac{\partial u}{\partial y} + w \frac{\partial u}{\partial z} \right) \frac{\partial T}{\partial x} \\ &\quad + \left(u \frac{\partial v}{\partial x} + v \frac{\partial v}{\partial y} + w \frac{\partial v}{\partial z} \right) \frac{\partial T}{\partial y} + \left(u \frac{\partial w}{\partial x} + v \frac{\partial w}{\partial y} + w \frac{\partial w}{\partial z} \right) \\ &\quad \left. \frac{\partial T}{\partial z} \right]. \end{aligned} \quad (1.27)$$

1.5 Homotopy Analysis Method (HAM)

1.5.1 Background

Most phenomena in nature are described by non-linear differential equations. These equations are much more difficult to solve than the linear ones. Traditional perturbation and asymptotic techniques are applied to obtain analytic approximations of these non-linear problems. Generally, these techniques strongly rely on small/large parameters which often make them valid for only weak non-linear problems. In 1992, Liao [37] presented an effective analytic technique known as homotopy analysis method (HAM) which has no such type of limitations and valid for strongly non-linear problems. HAM provides us a convenient way to control the convergence of series solutions. The basic idea of HAM is explained below:

1.5.2 Basic idea of HAM

Consider a differential equation

$$\mathcal{N}[f(\eta)] = 0, \quad (1.28)$$

where \mathcal{N} is the non-linear operator, η is the independent variable and $f(\eta)$ is the unknown function.

Suppose $\phi_m(\eta)|_{\eta \geq 0}$ is a set of functions such that $f(\eta)$ can be expressed in the form of series is

$$f(\eta) = \sum_{m=0}^{\infty} c_m \phi_m(\eta), \quad (1.29)$$

in which c_m are coefficients. The auxiliary linear operator \mathcal{L} is chosen as

$$\mathcal{L}[w(\eta)] = 0, \quad (1.30)$$

where $w(\eta)$ can also be written by

$$w(\eta) = \sum_{m=0}^{m_1} b_k \phi_m(\eta). \quad (1.31)$$

(a) Zeroth order deformation equation

Let $q \in [0, 1]$ be an embedding parameter and \hbar be the non-zero auxiliary parameter, then zeroth-order deformation problem for Eq. (1.28) can be expressed as

$$(1 - q)\mathcal{L}[\hat{f}(\eta; q) - f_0(\eta)] = q\hbar\mathcal{N}[\hat{f}(\eta; q)], \quad (1.32)$$

with the initial condition

$$\hat{f}(0; q) = 0. \quad (1.33)$$

It is easy to note that when $q = 0$, Eq. (1.32) gives the initial guess $f_0(\eta)$ while final solution is recovered by setting $q = 1$ i.e

$$\hat{f}(\eta; 0) = f_0(\eta), \quad (1.34)$$

$$\hat{f}(\eta; 1) = f(\eta). \quad (1.35)$$

Now we expand $\hat{f}(\eta; q)$ by using Taylor series about $q = 0$ as

$$\hat{f}(\eta; q) = \sum_{m=0}^{\infty} \frac{1}{m!} \left. \frac{\partial^m \hat{f}(\eta; q)}{\partial q^m} \right|_{q=0} q^m. \quad (1.36)$$

Assuming that series (1.36) converges at $q = 1$, we get

$$f(\eta) = f_0(\eta) + \sum_{m=1}^{\infty} f_m(\eta). \quad (1.37)$$

(b) m th-order deformation equation

Now differentiating the Eq. (1.32) m -times and then setting $q = 0$, one arrive at the following set of equations

$$\mathcal{L}_f[f_m(\eta) - \chi_m f_{m-1}(\eta)] = \hbar R_m^f(\eta), \quad m = 1, 2, 3, \dots, m-1 \quad (1.38)$$

where

$$R_m^f(\eta) = \frac{1}{(m-1)!} \left. \frac{\partial^{m-1} \mathcal{N}(\hat{f}(\eta; q))}{\partial p^{m-1}} \right|_{p=0} \quad (1.39)$$

$$\chi_m = \begin{cases} 0, & \text{if } m \leq 1 \\ 1, & \text{if } m > 1. \end{cases} \quad (1.40)$$

1.6 Literature survey

The phenomenon of heat transfer has widespread industrial and bio-medical applications such as cooling of electronic devices, nuclear reactor cooling, power generation, heat conduction in tissues and many others. The heat flux model proposed by Fourier [1] has been the most successful model for understanding heat transfer mechanism in diverse situations. One of the limitations of this model is that it often leads to a parabolic energy equation which indicates that initial disturbance is instantly experienced by the medium under consideration. This physically unrealistic feature is referred in the literature as ‘‘Paradox of heat conduction’’. In order to overcome this enigma, various researchers have proposed alterations in the Fourier’s heat conduction law. Cattaneo [2] modified this law through the inclusion of thermal relaxation time which is defined as the time required establishing heat

conduction once the temperature gradient is imposed. Christov [3] further modified the Cattaneo model by replacing the ordinary derivative with the Oldroyd's upper-convected derivative. He also presented the energy equation for arbitrary velocity and temperature fields. Straughan [4] applied Cattaneo-Christov model to study thermal convection in horizontal layer of incompressible Newtonian fluid under the influence of gravity. Ciarletta and Straughan [5] proved the uniqueness and stability of the solutions for the Cattaneo-Christov equations. Tibullo and Zampoli [6] investigated the uniqueness of solutions for an incompressible flow problem by using Cattaneo-Christov model. Han et al. [7] considered the two-dimensional flow and heat transfer of viscoelastic fluid over a stretching sheet using the Cattaneo-Christov heat flux model. In this study the analytic solutions were achieved by homotopy analysis method (HAM). Mustafa [8] developed both numerical and homotopy solutions for rotating flow of Maxwell fluid through Cattaneo-Christov theory. Later, Khan et al. [9] presented numerical approximations for viscoelastic flow over an exponentially stretching surface with the consideration of Cattaneo-Christov model. In a recent paper Hayat et al. [10] discussed the impact of Cattaneo-Christov heat conduction on the flow problem involving oldroyd-B fluid.

The analysis of magnetohydrodynamic (MHD) in viscous or non-newtonian flow is important in MHD generators, plasma studies, thermal therapy for cancer treatment, contrast enhancement in magnetic resonance imaging (MRI), nuclear reactors, geothermal energy extraction and many others. More precisely, MHD flow caused by the deformation of the walls of vessel containing the fluid has special value in modern metallurgical and metal working processes. Several recent attempts have been put forward in this direction in which Zheng et al. [11] studied the velocity slip and temperature jump conditions for MHD flow and heat transfer due to shrinking surface. Mixed convection flow of nanofluid under the influence of magnetic force

was numerically explored by Dhanai et al. [12]. Mabood et al. [13] describe the influence of magnetic field on the nanofluid flow driven by a non-linearly stretching surface. Second order slip effects on the boundary layer flow of nanofluid adjacent to stretching/shrinking sheet were discussed by Abdul Hakeem et al. [14]. Rashidi et al. [15] numerically explored the magnetic field effects on mixed convection flow of nanofluid in a vertical channel having sinusoidal walls. Hayat et al. [16] analytically investigates the peristaltic transport of in inclined channel under inclined magnetic field effects. In another paper Hayat et al. [17] discussed the MHD peristaltic motion of nanofluid in complaint wall channel.

Present work is undertaken to study the heat transfer in MHD three-dimensional flow of upper-convected Maxwell fluid by using Cattaneo-Christov heat flux model. Maxwell fluid is one of the popular viscoelastic models that can address the influence of fluid relaxation time. The boundary layer flows of Maxwell fluid have received remarkable attention in the past. Some interesting flow problems involving Maxwell fluid can be found in refs. [18-27]. The equations are formulated and then solved for convergence of series solution by homotopic approach. Graphs are sketched to see the influence of important parameters on the velocity and temperature fields.

Chapter 2

Stagnation point flow of an upper-convected Maxwell (UCM) fluid with mass transfer

This chapter is the review of an article by Hayat et al. [38]. This chapter deals with the effects of mass transfer due to stagnation point flow of an upper-convected Maxwell (UCM) fluid. The analytical solutions for velocity and concentration fields are obtained by homotopy analysis method (HAM). Suitable values of the convergence control parameters are selected by plotting the so-called h -curves. Influence of parameters appearing in the solution is examined graphically.

2.1 Problem formulation

Consider a steady and incompressible stagnation point flow of an upper-convected Maxwell (UCM) fluid bounded by a stretching surface at $y = 0$. Fluid occupies the region $y \geq 0$. A uniform magnetic field of strength B_0 is taken into account in transverse direction. The concentration at the sheet surface is c_w , while c_∞ denote

the concentration rate far away from the sheet and k_1 is the constant reaction rate. The component of free stream velocity are as below:

$$u = u_e(x) = ax, \quad v_e(y) = -ay \quad (2.1)$$

Let $u_w(x) = cx$ be the velocity of the stretching sheet. The boundary layer equations governing the flow and mass transfer of upper-convected Maxwell (UCM) fluid are as below:

$$\frac{\partial u}{\partial x} + \frac{\partial v}{\partial y} = 0, \quad (2.2)$$

$$\frac{\partial u}{\partial x} + v \frac{\partial u}{\partial y} + \lambda_1 \left[u^2 \frac{\partial^2 u}{\partial x^2} + v^2 \frac{\partial^2 u}{\partial y^2} + 2uv \frac{\partial^2 u}{\partial x \partial y} \right] = \nu \frac{\partial^2 u}{\partial y^2} + u_e \frac{du_e}{dx} - \frac{\sigma B_0^2}{\rho} \left(u - u_e + \lambda_1 v \frac{\partial u}{\partial y} \right), \quad (2.3)$$

$$u \frac{\partial C}{\partial x} + v \frac{\partial C}{\partial y} = D \frac{\partial^2 C}{\partial y^2} - k_1 C. \quad (2.4)$$

where u and v are the velocity components along the x - and y - directions respectively, ρ is the fluid density, λ_1 is the fluid relaxation time, ν is the kinematic viscosity and D is the mass diffusion, C is the concentration field and k_1 is the reaction rate. The body force due to the applied magnetic field is taken from [28-36]. The boundary conditions of the above problem are

$$\begin{aligned} u = u_w = cx, \quad v = 0, \quad C = C_w \quad \text{at } y = 0, \\ u \rightarrow u_e(x) = ax, \quad C \rightarrow C_\infty \quad \text{as } y \rightarrow \infty \end{aligned} \quad (2.5)$$

Considering the following similarity transformations [28, 30, 32, 34, 36]

$$\eta = \sqrt{\frac{c}{v}} y, \quad u = cx f'(\eta), \quad v = -\sqrt{cv} f(\eta), \quad \phi = \frac{C - C_\infty}{C_w - C_\infty}. \quad (2.6)$$

The Eqs. (2.3)-(2.5) can be reduced to the following system of ODEs.

$$f''' - M^2(f' - \alpha) + (M^2\beta + 1)ff'' - f'^2 + \alpha^2 + \beta(2ff'f'' - f^2f''') = 0, \quad (2.7)$$

$$\phi'' + Scf\phi' - Sc\gamma\phi = 0, \quad (2.8)$$

$$\begin{aligned}
f &= 0, \quad f' = 1, \quad \phi = 1 \quad \text{at} \quad \eta = 0, \\
f' &= \alpha, \quad \phi = 0 \quad \text{as} \quad \eta \rightarrow \infty,
\end{aligned} \tag{2.9}$$

so

$$M^2 = \frac{\sigma B_0^2}{\rho c}, \quad \beta = \lambda_1 c, \quad \alpha = \frac{a}{c}, \quad Sc = \frac{\nu}{D}, \quad \gamma = \frac{K_1}{c}. \tag{2.10}$$

Here M , γ and Sc denote the Hartman number, chemical reaction parameter and Schmidt number respectively. The Deborah number β appears here due to the presence relaxation time λ_1 . We now define the local Sherwood number as

$$Sh = \frac{x j_w}{D(C_w - C_\infty)}, \tag{2.11}$$

in which j_w is the wall mass flux given by

$$j_w = -D \left(\frac{\partial C}{\partial y} \right)_{y=0}, \tag{2.12}$$

In dimensionless form we have,

$$Sh/Re_x^{\frac{1}{2}} = -\phi'(0). \tag{2.13}$$

2.2 Series solutions

In this section, we deal with the series solutions by homotopy analysis method (HAM) [37] for non-linear system of equations (2.7) and (2.8) with boundary conditions (2.9).

In order to proceed, we choose initial approximations for functions f_0 and ϕ_0 as follows:

$$f_0(\eta) = \alpha\eta + (1 - \alpha)(1 - e^{-\eta}), \tag{2.14}$$

$$\phi_0(\eta) = e^{-\eta},$$

The auxiliary linear operators are selected as

$$\mathcal{L}_f(f) = f''' - f', \quad (2.15)$$

$$\mathcal{L}_\phi(\phi) = \phi'' - \phi,$$

where

$$\mathcal{L}_f(C_1 + C_2e^\eta + C_3e^{-\eta}) = 0, \quad (2.16)$$

$$\mathcal{L}_\phi(C_4e^\eta + C_5e^{-\eta}) = 0$$

where $C_i (i = 1 \dots 5)$ are the arbitrary constants. If $p \in [0, 1]$ is an embedding parameter, \hbar is the non-zero convergence control parameter then zeroth-order deformation problems can be constructed as

$$(1 - p)\mathcal{L}_f[\hat{f}(\eta; p) - f_0(\eta)] = p\hbar\mathcal{N}_f[\hat{f}(\eta; p)], \quad (2.17)$$

$$(1 - p)\mathcal{L}_\phi[\hat{\phi}(\eta; p) - \phi_0(\eta)] = p\hbar\mathcal{N}_\phi[\hat{f}(\eta; p), \hat{\phi}(\eta; p)], \quad (2.18)$$

$$\hat{f}(\eta; p) \Big|_{\eta=0} = 0, \quad \frac{\partial \hat{f}(\eta; p)}{\partial \eta} \Big|_{\eta=0} = 1, \quad \frac{\partial \hat{f}(\eta; p)}{\partial \eta} \Big|_{\eta \rightarrow \infty} = \alpha, \quad (2.19)$$

$$\hat{\phi}(\eta; p) \Big|_{\eta=0} = 1, \quad \hat{\phi}(\eta; p) \Big|_{\eta \rightarrow \infty} = 0.$$

Now consider the non-linear operators \mathcal{N}_f and \mathcal{N}_ϕ as below:

$$\begin{aligned} \mathcal{N}_f[\hat{f}(\eta; p)] &= \frac{\partial^3 \hat{f}(\eta; p)}{\partial \eta^3} - M^2 \left(\frac{\partial \hat{f}(\eta; p)}{\partial \eta} - \alpha \right) + (M^2\beta + 1)\hat{f}(\eta; p) \frac{\partial^2 \hat{f}(\eta; p)}{\partial \eta^2} - \\ &\left(\frac{\partial \hat{f}(\eta; p)}{\partial \eta} \right)^2 + \alpha^2 + \beta \left(2\hat{f}(\eta; p) \frac{\partial \hat{f}(\eta; p)}{\partial \eta} \frac{\partial^2 \hat{f}(\eta; p)}{\partial \eta^2} - \hat{f}^2(\eta; p) \frac{\partial^3 \hat{f}(\eta; p)}{\partial \eta^3} \right), \end{aligned} \quad (2.20)$$

$$\mathcal{N}_\phi \left[\hat{f}(\eta; p), \hat{\phi}(\eta; p) \right] = \frac{\partial^2 \hat{\phi}(\eta; p)}{\partial \eta^2} + Sc\hat{f}(\eta; p) \frac{\partial \hat{\phi}(\eta; p)}{\partial \eta} - Sc\gamma \hat{\phi}(\eta; p), \quad (2.21)$$

The zeroth-order deformation problems for $p = 0$ and $p = 1$ in Eqs. (2.17)-(2.19) have the following form.

$$\begin{aligned}\hat{f}(\eta; 0) &= f_0(\eta), & \hat{f}(\eta; 1) &= f(\eta), \\ \hat{\phi}(\eta; 0) &= \phi_0(\eta), & \hat{\phi}(\eta; 1) &= \phi(\eta).\end{aligned}\tag{2.22}$$

Now utilizing Taylor series expansion we have

$$\hat{f}(\eta; p) = f_0(\eta) + \sum_{m=1}^{\infty} f_m(\eta) p^m,\tag{2.23}$$

$$\hat{\phi}(\eta; p) = \phi_0(\eta) + \sum_{m=1}^{\infty} \phi_m(\eta) p^m,\tag{2.24}$$

where,

$$f_m(\eta) = \frac{1}{m!} \left. \frac{\partial^m \hat{f}(\eta; p)}{\partial p^m} \right|_{p=0}, \quad \phi_m(\eta) = \frac{1}{m!} \left. \frac{\partial^m \hat{\phi}(\eta; p)}{\partial p^m} \right|_{p=0}.\tag{2.25}$$

The non-zero auxiliary parameter \hbar can be chosen in such a way that the series (2.23) and (2.24) converges at $p = 1$. Substituting $p = 1$ in Eqs. (2.23) and (2.24) we get

$$f(\eta) = f_0(\eta) + \sum_{m=1}^{\infty} f_m(\eta),\tag{2.26}$$

$$\phi(\eta) = \phi_0(\eta) + \sum_{m=1}^{\infty} \phi_m(\eta).\tag{2.27}$$

The m th-order deformation problems are

$$\mathcal{L}_f[f_m(\eta) - \chi_m f_{m-1}(\eta)] = \hbar R_m^f(\eta),\tag{2.28}$$

$$\mathcal{L}_\phi[\phi_m(\eta) - \chi_m \phi_{m-1}(\eta)] = \hbar R_m^\phi(\eta),$$

$$f_m(0) = f'_m(0) = f'_m(\infty) = 0,\tag{2.29}$$

$$\phi_m(0) = \phi_m(\infty) = 0,$$

$$R_m^f = f_{m-1}''' - M^2 \left(f_{m-1}' - \beta \sum_{k=0}^{m-1} [f_{m-k-1} f_k''] \right) + (1 - \chi_m)(\alpha M^2 + \alpha^2) \quad (2.30)$$

$$+ \sum_{k=0}^{m-1} [f_{m-k-1} f_k'' - f_{m-k-1}' f_k'] + \beta \sum_{k=0}^{m-1} f_{m-k-1} \sum_{l=0}^k [2f_{k-1}' f_l'' - f_{k-1} f_l'''],$$

$$R_m^\phi = \phi_{m-1}'' - Sc\gamma\phi_{m-1} + Sc \sum_{k=0}^{m-1} \phi_{m-k-1}' f_k, \quad (2.31)$$

$$\chi_m = \begin{cases} 0, & \text{if } m \leq 1, \\ 1, & \text{if } m > 1. \end{cases} \quad (2.32)$$

The general solutions are

$$f_m(\eta) = f_m^*(\eta) + C_1 + C_2 e^\eta + c_3 e^{-\eta}, \quad (2.33)$$

$$\phi_m(\eta) = \phi_m^*(\eta) + C_4 e^\eta + C_5 e^{-\eta}, \quad (2.34)$$

where f_m^* and ϕ_m^* denote the particular solutions of (2.29), the constants $C_i (i = 1 \dots 5)$ are defined by

$$C_2 = C_4 = 0, \quad C_3 = \left. \frac{\partial f_m^*(\eta)}{\partial \eta} \right|_{\eta=0}, \quad (2.35)$$

$$C_1 = -C_3 - f_m^*(0), \quad C_5 = -\phi_m^*(0). \quad (2.36)$$

2.3 Convergence of homotopy solutions

The non-zero auxiliary parameter \hbar in the analytic series solutions of Eqs. (2.26) and (2.27) plays an important role in controlling the convergence of homotopic series solutions. \hbar -curves are plotted at 15th-order of approximations to find the appropriate value of \hbar for which series solutions are convergent. The convergence series solutions are only possible in the range of $-0.6 \leq \hbar \leq -0.3$. Table 2.1 shows the convergence rate of the series solutions when $\alpha = 0.2$, $M = 1$, $Sc = 1 = \gamma$ and $\beta = 0.2$.

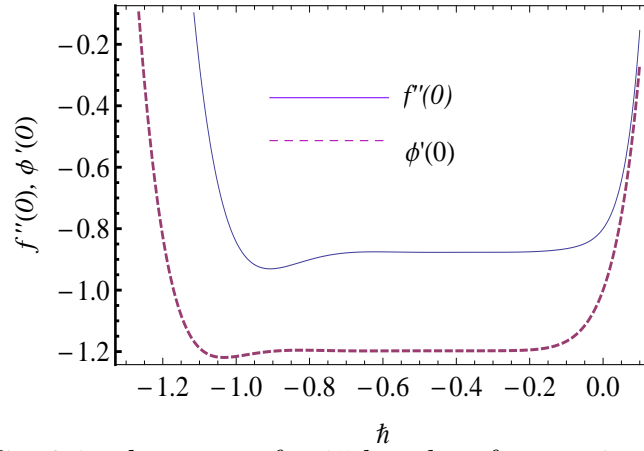


Fig. 2.1 – h - curves for 15th-order of approximations.

Order of approximation	$-f''(0)$	$-\phi'(0)$
1	1.160640	1.160640
2	1.232442	1.146636
5	1.270624	1.166805
10	1.272458	1.167852
15	1.272465	1.167858
20	1.272469	1.167860
25	1.272469	1.167860
30	1.272469	1.167860
40	1.272469	1.167860
50	1.272469	1.167860

Table 2.1 – Convergence of homotopy series solutions for different orders of approximations when $\alpha = 0.2$, $M = 1$, $Sc = 1 = \gamma$, $\beta = 0.2$ and $h = -0.7$.

2.4 Results and discussion

In this section, we present the effects of parameters on the velocity field f' and concentration field ϕ . For this purpose, the graphical results are presented in Fig. (2.2)-Fig. (2.9). Figs. (2.2) and (2.3) depict the behavior of α and M on f' . It is noticed that velocity and boundary-layer thickness are increasing function of α , whereas the velocity and boundary-layer thickness decrease when M is increased. Figs. (2.4) and (2.5) depict the behavior of Deborah number β on velocity field f' and concentration field ϕ respectively. It can be seen that fluid velocity decreases upon increasing the parameter β . However concentration ϕ is found to increase upon increasing β .

In Figs. (2.6) and (2.7) influence of M and Sc on concentration field ϕ is examined. Concentration ϕ appears to increase upon increasing the strength of magnetic force. The behaviors of Schmidt number Sc on ϕ is qualitative similar to that of M . The behavior of generative and destructive chemical reaction parameter are sketched in Figs. (2.8) and (2.9). We noticed that the concentration field ϕ increases/decreases when generative/destructive chemical reactor parameter is increased. Concentration distribution is much sensitive to the generative chemical reaction parameter. The values of surface mass transfer $-\phi'(0)$ are presented in the Table 2.2

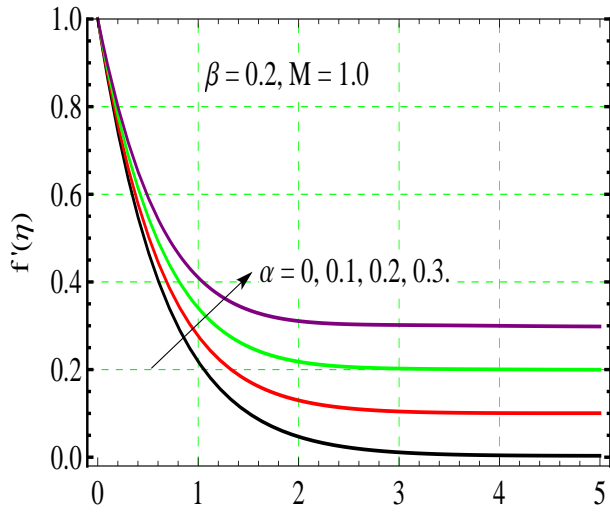


Fig. 2.2 – Variation of α on $f'(\eta)$.

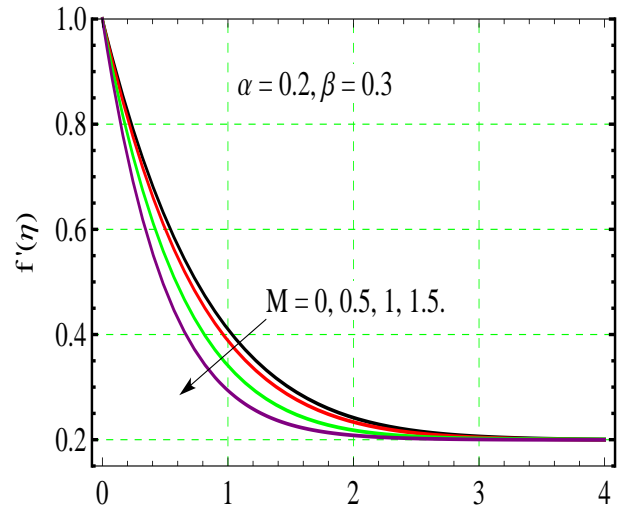


Fig. 2.3 – Variation of M on $f'(\eta)$.

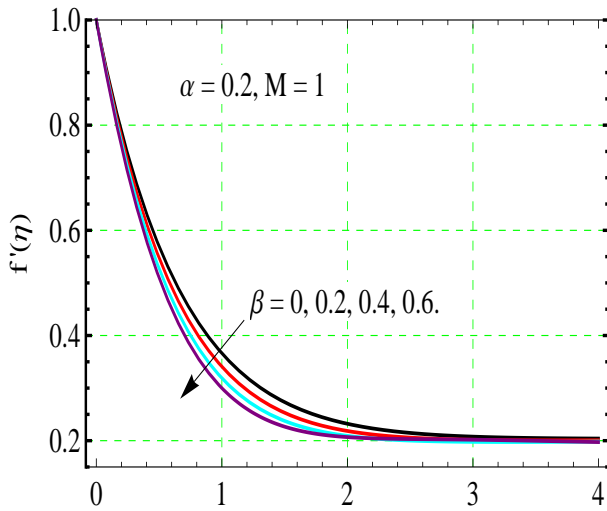


Fig. 2.4 – Variation of β on $f'(\eta)$.

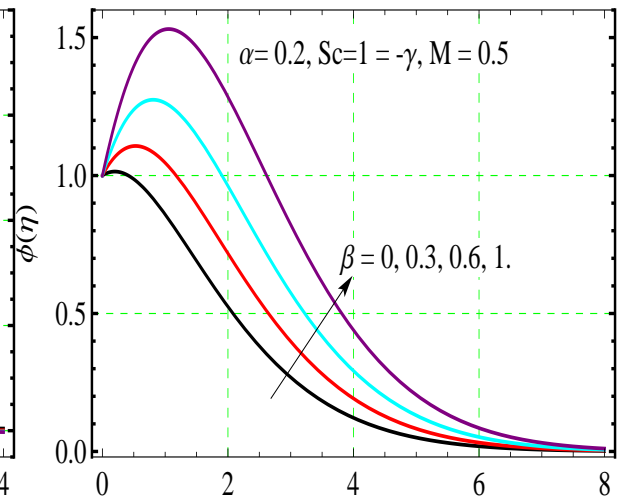


Fig. 2.5 – Variation of β on $\phi(\eta)$.

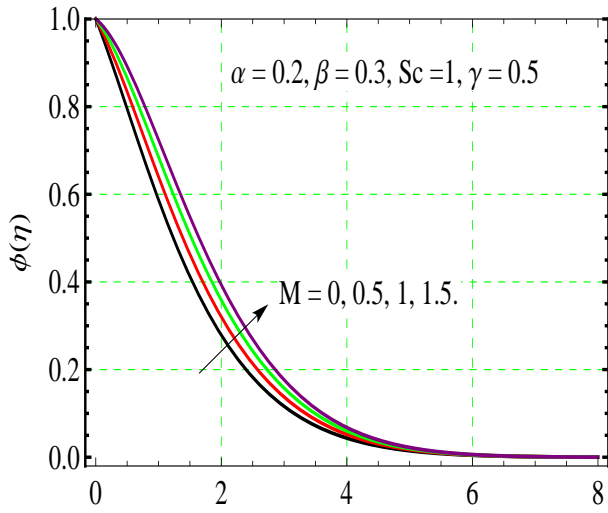


Fig. 2.6 – Variation of M on $\phi(\eta)$.

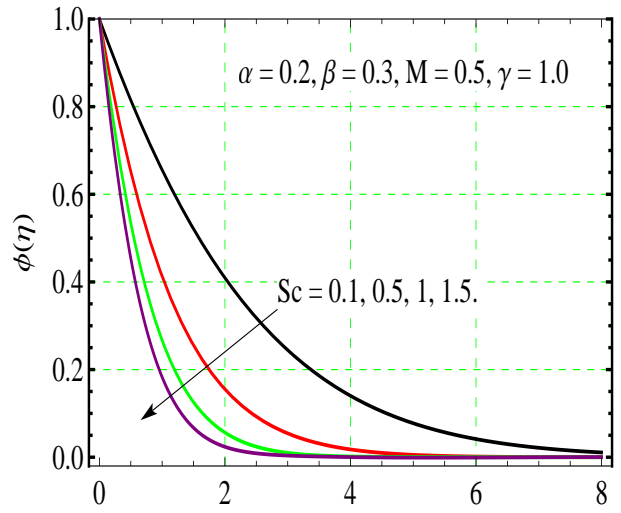


Fig. 2.7 – Variation of Sc on $\phi(\eta)$.

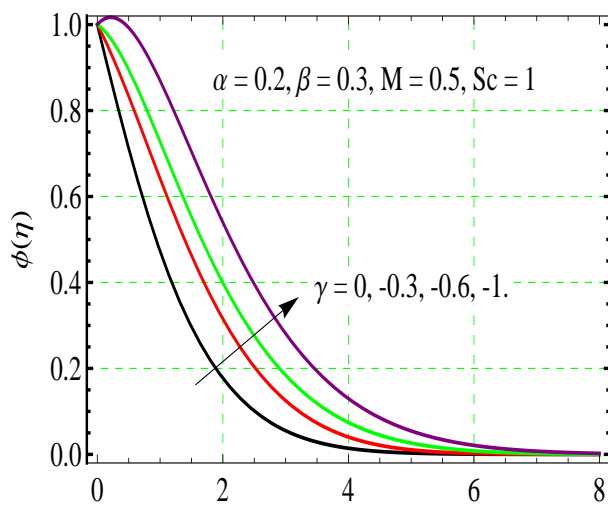


Fig. 2.8 – Variation of $\gamma < 0$ on $\phi(\eta)$.

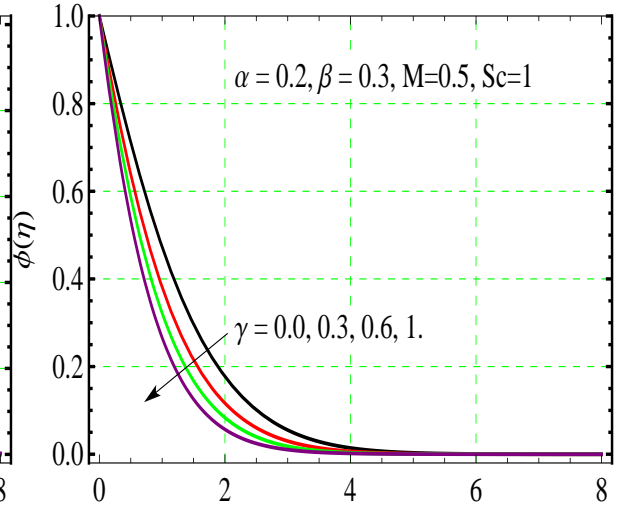


Fig. 2.9 – Variation of $\gamma > 0$ on $\phi(\eta)$.

α	M	β	$-\phi'(0)$
0.0	1.0	0.2	1.15092
0.2			1.16815
0.4			1.18727
0.7			1.22675
0.2	0.0		1.18142
	0.3		1.17980
	0.7		1.17385
	1.2		1.16351
	1.5		1.15680
	1.0	0.0	1.17169
		0.4	1.16524
		0.7	1.15125
		1.0	1.15505

Table 2.2 – Values of surface mass transfer $-\phi'(0)$ when $Sc = 1.0 = \gamma$.

Chapter 3

MHD three-dimensional flow of upper-convected Maxwell fluid using Cattaneo-Christov heat flux model

Here we consider the MHD three-dimensional flow of upper-convected Maxwell (UCM) fluid due to bi-directional stretching surface by considering the Cattaneo-Christov heat flux model. Cattaneo-Christov heat flux model is employed to investigate heat transfer process.

3.1 Problem formulation

Consider the flow of upper-convected Maxwell fluid induced by an elastic sheet stretching in two lateral directions. The sheet is coincident with the plane $z = 0$, whereas the fluid occupies the region $z \geq 0$. The electric field is absent while induced magnetic field is neglected due to the consideration of small magnetic Reynolds

number. The velocities of the stretching sheet along the x - and y - directions are $u_w(x) = ax$ and $v_w(y) = by$ respectively. The sheet is kept at constant temperature T_w , whereas T_∞ is the ambient value of the temperature such that $T_w > T_\infty$. Considering the velocity vector $V = [u(x, y, z), v(x, y, z), w(x, y, z)]$ and the temperature T the boundary layer equations for three-dimensional flow and heat transfer of Maxwell fluid can be expressed as below:

$$\frac{\partial u}{\partial x} + \frac{\partial v}{\partial y} + \frac{\partial w}{\partial z} = 0, \quad (3.1)$$

$$\begin{aligned} u \frac{\partial u}{\partial x} + v \frac{\partial u}{\partial y} + w \frac{\partial u}{\partial z} &= \nu \frac{\partial^2 u}{\partial z^2} - \lambda_1 \left(u^2 \frac{\partial^2 u}{\partial x^2} + v^2 \frac{\partial^2 u}{\partial y^2} + w^2 \frac{\partial^2 u}{\partial z^2} + 2uv \frac{\partial^2 u}{\partial x \partial y} \right. \\ &\quad \left. + 2vw \frac{\partial^2 u}{\partial y \partial z} + 2uw \frac{\partial^2 u}{\partial x \partial z} \right) - \frac{\sigma B_0^2}{\rho} \left(u + \lambda_1 w \frac{\partial u}{\partial z} \right), \end{aligned} \quad (3.2)$$

$$\begin{aligned} u \frac{\partial v}{\partial x} + v \frac{\partial v}{\partial y} + w \frac{\partial v}{\partial z} &= \nu \frac{\partial^2 v}{\partial z^2} - \lambda_1 \left(u^2 \frac{\partial^2 v}{\partial x^2} + v^2 \frac{\partial^2 v}{\partial y^2} + w^2 \frac{\partial^2 v}{\partial z^2} + 2uv \frac{\partial^2 v}{\partial x \partial y} \right. \\ &\quad \left. + 2vw \frac{\partial^2 v}{\partial y \partial z} + 2uw \frac{\partial^2 v}{\partial x \partial z} \right) - \frac{\sigma B_0^2}{\rho} \left(v + \lambda_1 w \frac{\partial v}{\partial z} \right), \end{aligned} \quad (3.3)$$

$$\rho c_p \left(u \frac{\partial T}{\partial x} + v \frac{\partial T}{\partial y} + w \frac{\partial T}{\partial z} \right) = -\nabla \cdot \mathbf{q}, \quad (3.4)$$

where u , v and w are the velocity components along the x -, y - and z - directions respectively, ν is the kinematic viscosity, c_p is the specific heat, σ is the electrical conductivity, ρ is the fluid density, T is the fluid temperature, λ_1 is the fluid relaxation time and \mathbf{q} is the heat flux which satisfies the following relationship [3].

$$\mathbf{q} + \lambda_2 \left[\frac{\partial \mathbf{q}}{\partial t} + \mathbf{V} \cdot \nabla \mathbf{q} - \mathbf{q} \cdot \nabla \mathbf{V} + (\nabla \cdot \mathbf{V}) \mathbf{q} \right] = -k \nabla T, \quad (3.5)$$

in which λ_2 is the thermal relaxation time and k is the thermal conductivity of the fluid. Following Christov [3], we eliminate \mathbf{q} from Eq. (3.4) and Eq. (3.5) to obtain

the following:

$$\begin{aligned}
u \frac{\partial T}{\partial x} + v \frac{\partial T}{\partial y} + w \frac{\partial T}{\partial z} &= \frac{k}{\rho c_p} \frac{\partial^2 T}{\partial z^2} - \lambda_2 \left[u^2 \frac{\partial^2 T}{\partial x^2} + v^2 \frac{\partial^2 T}{\partial y^2} + w^2 \frac{\partial^2 T}{\partial z^2} + 2uv \frac{\partial^2 T}{\partial x \partial y} + \right. \\
& 2vw \frac{\partial^2 T}{\partial y \partial z} + 2uw \frac{\partial^2 T}{\partial x \partial z} + \left. \left(u \frac{\partial u}{\partial x} + v \frac{\partial u}{\partial y} + w \frac{\partial u}{\partial z} \right) \frac{\partial T}{\partial x} + \left(u \frac{\partial v}{\partial x} + v \frac{\partial v}{\partial y} + w \frac{\partial v}{\partial z} \right) \frac{\partial T}{\partial y} + \left(u \frac{\partial w}{\partial x} + v \frac{\partial w}{\partial y} + w \frac{\partial w}{\partial z} \right) \frac{\partial T}{\partial z} \right] \quad (3.6)
\end{aligned}$$

Boundary conditions for the present problem are:

$$\begin{aligned}
u = u_w(x) = ax, \quad v = v_w(y) = by, \quad w = 0, \quad T = T_w \quad \text{at} \quad z = 0, \\
u \rightarrow 0, \quad v \rightarrow 0, \quad T \rightarrow T_\infty \quad \text{as} \quad z \rightarrow \infty.
\end{aligned} \quad (3.7)$$

Considering the following similarity transformations

$$\begin{aligned}
\eta = \sqrt{\frac{a}{\nu}} z, \quad u = ax f'(\eta), \quad v = ay g'(\eta), \quad w = -\sqrt{av} [f(\eta) + g(\eta)], \\
\theta = \frac{T - T_\infty}{T_w - T_\infty}.
\end{aligned} \quad (3.8)$$

Eq. (3.1) is identically satisfied and Eq. (3.2), Eq. (3.3), Eq. (3.6) and Eq. (3.7) take the following forms:

$$f'''' + (M^2 \beta + 1)(f + g)f'' - f'^2 + \beta \left[2(f + g)f'f'' - (f + g)^2 f'''' \right] - M^2 f' = 0, \quad (3.9)$$

$$g'''' + (M^2 \beta + 1)(f + g)g'' - g'^2 + \beta \left[2(f + g)g'g'' - (f + g)^2 g'''' \right] - M^2 g' = 0, \quad (3.10)$$

$$\frac{1}{Pr} \theta'' + (f + g)\theta' - \gamma \left[(f + g)(f' + g')\theta' + (f + g)^2 \theta'' \right] = 0, \quad (3.11)$$

$$\begin{aligned}
f(0) = g(0) = 0, \quad f'(0) = 1, \quad g'(0) = \lambda, \quad \theta(0) = 1, \\
f'(\infty) \rightarrow 0, \quad g'(\infty) \rightarrow 0, \quad \theta(\infty) \rightarrow 0,
\end{aligned} \quad (3.12)$$

where $\lambda = b/a$ is the ratio of the stretching rate along the y - direction to the stretching rate along the x - direction, $\beta = \lambda_1 a$ is the non-dimensional fluid relaxation time, $\gamma = \lambda_2 a$ is the non-dimensional relaxation time for heat flux and Pr is the Prandtl number. It can be noticed that when $\lambda = 0$, the two-dimensional case is jumped. Further $\lambda = 1$ corresponds to the case of axisymmetric flow.

3.2 Analytic solutions by homotopy analysis method

In this section, we deal with series solutions by homotopy analysis method (HAM) [28] for non-linear coupled equations (3.9), (3.10) and (3.11) with boundary conditions (3.12). In order to proceed, we choose initial approximations for functions f_0 , g_0 and θ_0 as follows:

$$f_0(\eta) = 1 - e^{-\eta}, \quad g_0(\eta) = \lambda(1 - e^{-\eta}), \quad \theta_0(\eta) = e^{-\eta}. \quad (3.13)$$

The auxiliary linear operators \mathcal{L}_f , \mathcal{L}_g and \mathcal{L}_θ are selected as

$$\mathcal{L}_f(\eta) = f''' - f', \quad \mathcal{L}_g(\eta) = g''' - g', \quad \mathcal{L}_\theta(\eta) = \theta'' - \theta. \quad (3.14)$$

Now consider the non-linear operators \mathcal{N}_f , \mathcal{N}_g and \mathcal{N}_θ as below:

$$\begin{aligned} \mathcal{N}_f[\hat{f}(\eta; p), \hat{g}(\eta; p)] &= \frac{\partial^3 \hat{f}(\eta; p)}{\partial \eta^3} - \left(\frac{\partial \hat{f}(\eta; p)}{\partial \eta} \right)^2 + (M^2 \beta + 1)(\hat{f}(\eta; p) + \hat{g}(\eta; p)) \\ &\quad \frac{\partial^2 \hat{f}(\eta; p)}{\partial \eta^2} + \beta \left(2(\hat{f}(\eta; p) + \hat{g}(\eta; p)) \frac{\partial \hat{f}(\eta; p)}{\partial \eta} \frac{\partial^2 \hat{f}(\eta; p)}{\partial \eta^2} - \right. \\ &\quad \left. (\hat{f}(\eta; p) + \hat{g}(\eta; p))^2 \frac{\partial^3 \hat{f}(\eta; p)}{\partial \eta^3} \right) - M^2 \frac{\partial \hat{f}(\eta; p)}{\partial \eta}, \end{aligned} \quad (3.15)$$

$$\begin{aligned} \mathcal{N}_g[\hat{g}(\eta; p), \hat{f}(\eta; p)] &= \frac{\partial^3 \hat{g}(\eta; p)}{\partial \eta^3} - \left(\frac{\partial \hat{g}(\eta; p)}{\partial \eta} \right)^2 + (M^2 \beta + 1)(\hat{f}(\eta; p) + \hat{g}(\eta; p)) \\ &\quad \frac{\partial^2 \hat{g}(\eta; p)}{\partial \eta^2} + \beta \left(2(\hat{f}(\eta; p) + \hat{g}(\eta; p)) \frac{\partial \hat{g}(\eta; p)}{\partial \eta} \frac{\partial^2 \hat{g}(\eta; p)}{\partial \eta^2} - \right. \\ &\quad \left. - (\hat{f}(\eta; p) + \hat{g}(\eta; p))^2 \frac{\partial^3 \hat{g}(\eta; p)}{\partial \eta^3} \right) - M^2 \frac{\partial \hat{g}(\eta; p)}{\partial \eta}, \end{aligned} \quad (3.16)$$

$$\begin{aligned}
\mathcal{N}_\theta[\hat{\theta}(\eta; p), \hat{f}(\eta; p), \hat{g}(\eta; p)] &= \frac{1}{Pr} \frac{\partial^2 \hat{\theta}(\eta; p)}{\partial \eta^2} + (\hat{f}(\eta; p) + \hat{g}(\eta; p)) \frac{\partial \hat{\theta}(\eta; p)}{\partial \eta} - \gamma \left((\hat{f}(\eta; p) \right. \\
&+ \hat{g}(\eta; p)) \left(\frac{\partial \hat{f}(\eta; p)}{\partial \eta} + \frac{\partial \hat{g}(\eta; p)}{\partial \eta} \right) \frac{\partial \hat{\theta}(\eta; p)}{\partial \eta} + (\hat{f}(\eta; p) + \\
&\left. \hat{g}(\eta; p))^2 \frac{\partial^2 \hat{\theta}(\eta; p)}{\partial \eta^2} \right). \tag{3.17}
\end{aligned}$$

The auxiliary linear operators in equation (3.14) satisfy the following:

$$\mathcal{L}_f(C_1 + C_2 e^\eta + C_3 e^{-\eta}) = 0, \quad \mathcal{L}_g(C_4 + C_5 e^\eta + C_6 e^{-\eta}) = 0, \quad \mathcal{L}_\theta(C_7 e^\eta + C_8 e^{-\eta}) = 0, \tag{3.18}$$

in which $C_i (i = 1 - 8)$ are constants.

Following the basic idea of HAM [28], we express the zeroth-order deformation problems for Eqs. (3.9)-(3.12) are listed as

$$(1 - p) \mathcal{L}_f \left[\hat{f}(\eta; p) - f_0(\eta) \right] = p \hbar \mathcal{N}_f \left[\hat{f}(\eta; p), \hat{g}(\eta; p) \right], \tag{3.19}$$

$$(1 - p) \mathcal{L}_g \left[\hat{g}(\eta; p) - g_0(\eta) \right] = p \hbar \mathcal{N}_g \left[\hat{f}(\eta; p), \hat{g}(\eta; p) \right], \tag{3.20}$$

$$(1 - p) \mathcal{L}_\theta \left[\hat{\theta}(\eta; p) - \theta_0(\eta) \right] = p \hbar \mathcal{N}_\theta \left[\hat{f}(\eta; p), \hat{g}(\eta; p), \hat{\theta}(\eta; p) \right]. \tag{3.21}$$

The boundary-conditions are

$$\begin{aligned}
\hat{f}(\eta; p) \Big|_{\eta=0} &= 0, & \frac{\partial \hat{f}(\eta; p)}{\partial \eta} \Big|_{\eta=0} &= 1, & \frac{\partial \hat{f}(\eta; p)}{\partial \eta} \Big|_{\eta \rightarrow \infty} &= 0, \\
\hat{g}(\eta; p) \Big|_{\eta=0} &= 0, & \frac{\partial \hat{g}(\eta; p)}{\partial \eta} \Big|_{\eta=0} &= \lambda, & \frac{\partial \hat{g}(\eta; p)}{\partial \eta} \Big|_{\eta \rightarrow \infty} &= 0, \\
\hat{\theta}(\eta; p) \Big|_{\eta=0} &= 1, & \hat{\theta}(\eta; p) \Big|_{\eta \rightarrow \infty} &= 0, & &
\end{aligned} \tag{3.22}$$

where $p \in [0, 1]$ is an embedding parameter and \hbar is the non-zero convergence control parameter. When $p = 0$ and $p = 1$ we have:

$$\begin{aligned}
\hat{f}(\eta; 0) &= f_0(\eta), & \hat{g}(\eta; 0) &= g_0(\eta), & \hat{\theta}(\eta; 0) &= \theta_0(\eta), \\
\hat{f}(\eta; 1) &= f(\eta), & \hat{g}(\eta; 1) &= g(\eta), & \hat{\theta}(\eta; 1) &= \theta(\eta).
\end{aligned} \tag{3.23}$$

Now expanding $\hat{f}(\eta; p)$, $\hat{g}(\eta; p)$ and $\hat{\theta}(\eta; p)$ in Taylor's series about $p = 0$.

$$\hat{f}(\eta; p) = f_0(\eta) + \sum_{m=1}^{\infty} f_m(\eta)p^m, \quad (3.24)$$

$$\hat{g}(\eta; p) = g_0(\eta) + \sum_{m=1}^{\infty} g_m(\eta)p^m, \quad (3.25)$$

$$\hat{\theta}(\eta; p) = \theta_0(\eta) + \sum_{m=1}^{\infty} \theta_m(\eta)p^m, \quad (3.26)$$

$$\begin{aligned} \hat{f}(\eta; p) \Big|_{\eta=0} &= 0, & \frac{\partial \hat{f}(\eta; p)}{\partial \eta} \Big|_{\eta=0} &= 1, & \frac{\partial \hat{f}(\eta; p)}{\partial \eta} \Big|_{\eta \rightarrow \infty} &= 0, \\ \hat{g}(\eta; p) \Big|_{\eta=0} &= 0, & \frac{\partial \hat{g}(\eta; p)}{\partial \eta} \Big|_{\eta=0} &= \lambda, & \frac{\partial \hat{g}(\eta; p)}{\partial \eta} \Big|_{\eta \rightarrow \infty} &= 0, \\ \hat{\theta}(\eta; p) \Big|_{\eta=0} &= 1, & \hat{\theta}(\eta; p) \Big|_{\eta \rightarrow \infty} &= 0. \end{aligned} \quad (3.27)$$

where

$$f_m(\eta) = \frac{1}{m!} \frac{\partial^m \hat{f}(\eta; p)}{\partial p^m} \Big|_{p=0}, \quad g_m(\eta) = \frac{1}{m!} \frac{\partial^m \hat{g}(\eta; p)}{\partial p^m} \Big|_{p=0}, \quad \theta_m(\eta) = \frac{1}{m!} \frac{\partial^m \hat{\theta}(\eta; p)}{\partial p^m} \Big|_{p=0}.$$

The auxiliary parameter \hbar can be chosen in such a way that the series (3.24)-(3.26) converges at $p = 1$. Substituting $p = 1$ in (3.24)-(3.26), we obtain

$$f(\eta) = f_0(\eta) + \sum_{m=1}^{\infty} f_m(\eta), \quad (3.28)$$

$$g(\eta) = g_0(\eta) + \sum_{m=1}^{\infty} g_m(\eta), \quad (3.29)$$

$$\theta(\eta) = \theta_0(\eta) + \sum_{m=1}^{\infty} \theta_m(\eta). \quad (3.30)$$

The problems at m th-order satisfy the following:

$$\mathcal{L}_f[f_m(\eta) - \chi_m f_{m-1}(\eta)] = \hbar R_m^f(\eta), \quad (3.31)$$

$$\mathcal{L}_g[g_m(\eta) - \chi_m g_{m-1}(\eta)] = \hbar R_m^g(\eta), \quad (3.32)$$

$$\mathcal{L}_\theta[\theta_m(\eta) - \chi_m \theta_{m-1}(\eta)] = \hbar R_m^\theta(\eta), \quad (3.33)$$

where

$$\begin{aligned} f_m(0) &= f'_m(0) = g_m(0) = g'_m(0) = \theta_m(0) = 0, \\ f'_m(\infty) &= g'_m(\infty) = \theta_m(\infty) = 0. \end{aligned} \quad (3.34)$$

Here

$$\begin{aligned} R_m^f(\eta) &= f'''_{m-1} + (M^2\beta + 1) \sum_{k=0}^{m-1} [(f_{m-1-k} + g_{m-1-k})f''_k - f'_{m-1-k}f'_k] + \beta \sum_{k=0}^{m-1} [2 \\ &\quad (f_{m-1-k} + g_{m-1-k}) \sum_{l=0}^k f'_{k-l}f''_l - (f_{m-1-k} \sum_{l=0}^k f_{k-l} + g_{m-1-k} \sum_{l=0}^k g_{k-l} + \\ &\quad 2f_{m-1-k} \sum_{l=0}^k g_{k-l})f'''_l] - M^2 f'_{m-1}, \end{aligned} \quad (3.35)$$

$$\begin{aligned} R_m^g(\eta) &= g'''_{m-1} + (M^2\beta + 1) \sum_{k=0}^{m-1} [(f_{m-1-k} + g_{m-1-k})g''_k - g'_{m-1-k}g'_k] + \beta \sum_{k=0}^{m-1} [2 \\ &\quad (f_{m-1-k} + g_{m-1-k}) \sum_{l=0}^k g'_{k-l}g''_l - (f_{m-1-k} \sum_{l=0}^k f_{k-l} + g_{m-1-k} \sum_{l=0}^k g_{k-l} + 2f_{m-1-k} \\ &\quad \sum_{l=0}^k g_{k-l})g'''_l] - M^2 g'_{m-1}, \end{aligned} \quad (3.36)$$

$$\begin{aligned} R_m^\theta(\eta) &= \frac{1}{Pr} \theta''_{m-1} + \sum_{k=0}^{m-1} [(f_{m-1-k} + g_{m-1-k})\theta'_k] - \gamma \sum_{k=0}^{m-1} [2(f_{m-1-k} + g_{m-1-k}) \\ &\quad \sum_{l=0}^k (f'_{k-l} + g'_{k-l})\theta'_l + (f_{m-1-k} \sum_{l=0}^k f_{k-l} + g_{m-1-k} \sum_{l=0}^k g_{k-l} + 2f_{m-1-k} \\ &\quad \sum_{l=0}^k g_{k-l})\theta''_l], \end{aligned} \quad (3.37)$$

$$\chi_m = \begin{cases} 0, & \text{if } m \leq 1 \\ 1, & \text{if } m > 1 \end{cases}.$$

3.3 Convergence of homotopy series solutions

Note that the series solutions given in (3.27)-(3.29) contain an auxiliary parameters \hbar which has an important role in controlling the convergence of homotopic solutions. To select an appropriate value of \hbar , we have plotted the so-called \hbar -curves for $f''(0)$, $g''(0)$ and $\theta'(0)$ in Fig. 3.1. Here the valid range of \hbar lies where the \hbar -curves are parallel to \hbar -axis. From Fig. 3.1, we expect that series solutions for f , g and θ would converge in the range $-1.5 \leq \hbar \leq -0.4$. Table 3.1 is plotted to see the convergence rate of the solutions. We observe that tenth-order approximations are sufficient for convergent solutions at $\hbar = -0.8$.

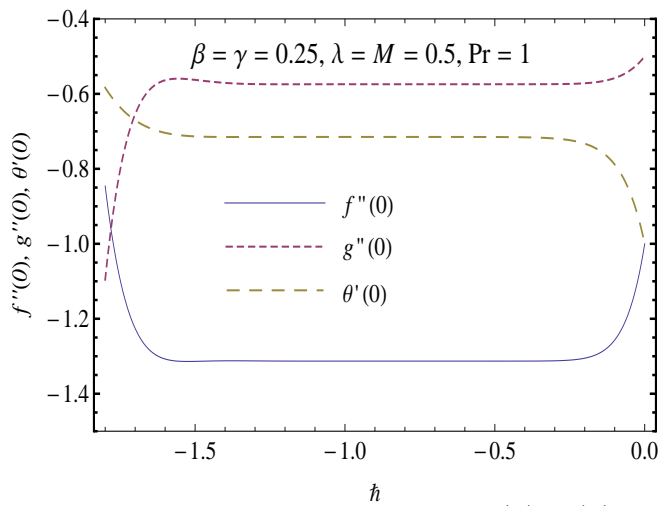


Fig. 3.1 – \hbar -curves for the functions $f(\eta)$, $g(\eta)$ and $\theta(\eta)$.

<i>Order of approximations</i>	$f''(0)$	$g''(0)$	$\theta'(0)$
5	-1.31282	-0.57423	-0.71696
10	-1.31296	-0.57435	-0.71497
15	-1.31296	-0.57435	-0.71492
20	-1.31296	-0.57435	-0.71491
25	-1.31296	-0.57435	-0.71491
30	-1.31296	-0.57435	-0.71491
35	-1.31296	-0.57435	-0.71491
40	-1.31296	-0.57435	-0.71491

Table 3.1 – Convergence of HAM solutions for different orders of approximations when $\beta = \gamma = 0.25$, $Pr = 1$, $M = \lambda = 0.5$ and $\hbar = -0.8$.

3.4 Results and discussion

This section focuses on the physical interpretation of the behaviour of the embedded parameters on the solutions. For this purpose, we display graphical results in Fig. 3.2- Fig. 3.11. Table 3.1 includes the numerical values of wall temperature gradient $\theta'(0)$ for different value of β , γ and M . The entries of this table are obtained at suitable choice of \hbar . It is observed that $\theta'(0)$ has direct relationship with the thermal relaxation time. However it is a decreasing function of the fluid relaxation time β . The presence of magnetic field also causes diminution in the magnitude of heat transfer rate from the surface.

The behavior of non-dimensional relaxation time β on both the u - and v - components of velocity can be observed from Fig. 3.2 and Fig. 3.3 respectively. The velocity profiles are tilted towards the wall when β is increased indicating that velocity and boundary layer thickness are decreasing function of β .

Physically, bigger β indicates stronger viscous force which restricts the fluid motion and consequently the velocity decreases. Fig. 3.4 and Fig. 3.5 show the impact of stretching rates ratio λ on the velocity fields f' and g' respectively. Bigger values of λ indicates larger rate of stretching along the v - direction compared to u - direction. Therefore, with an increase in λ , the velocity in the v - direction increases and velocity in the original u - direction decreases simultaneously.

In Fig. 3.6 and Fig. 3.7, the velocity distributions are presented for different value of Hartman number M . Velocities in both u - and v - directions decrease upon increasing the M . This decrease in the velocity is due to resistance offered by the Lorentz force acting in the normal direction. From Fig. 3.8, we observe that the resistance associated with Lorentz force supports the penetration depth of temperature.

In Fig. 3.9, the temperature profiles are presented for different Prandtl numbers. Here $\gamma = 0$ indicates the corresponding results for the classical Fourier law. Prandtl number has inverse relationship with thermal diffusivity. Therefore an increase in Pr reduces conduction and hence causes a reduction in the penetration depth of temperature. The results are qualitatively similar in both Fourier and Cattaneo-Christov heat flux models.

The effects of non-dimensional relaxation time γ on temperature distribution can be analyzed from Fig. 3.10. Temperature θ decreases and profiles smoothly descend to zero at shorter distance from the sheet when γ is incremented. This indicates that there will be thinner thermal boundary layer when relaxation time for heat flux is larger. Here the profiles become steeper in the vicinity of the boundary as γ

increases which is an indication of the growth in wall slope of temperature θ .

The impact of stretching rates ratio on the temperature distribution can be analyzed through Fig. 3.11. Although we do not include the results for entrainment velocity here but our computations indicate that entrainment velocity $f(\infty) + g(\infty)$ is an increasing function of λ . Due to this reason, an increase in λ enhances the intensity of the cold fluid at the ambient towards the hot stretching surface. Consequently the fluid temperature drops within the boundary layer, when λ is increased.

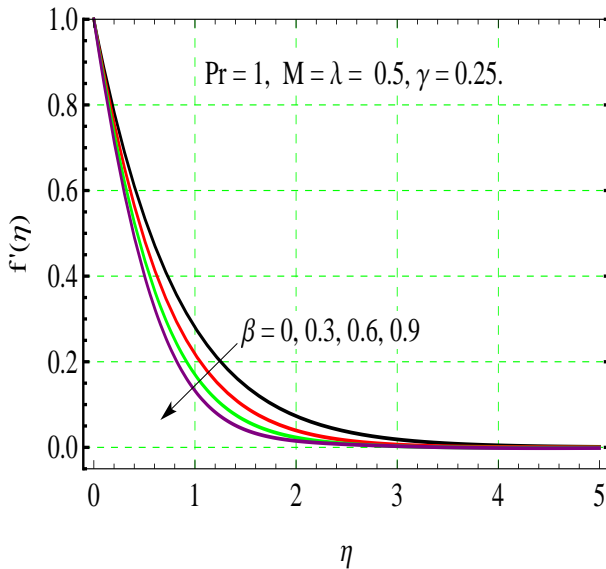


Fig. 3.2 – Effect of β on $f'(\eta)$.

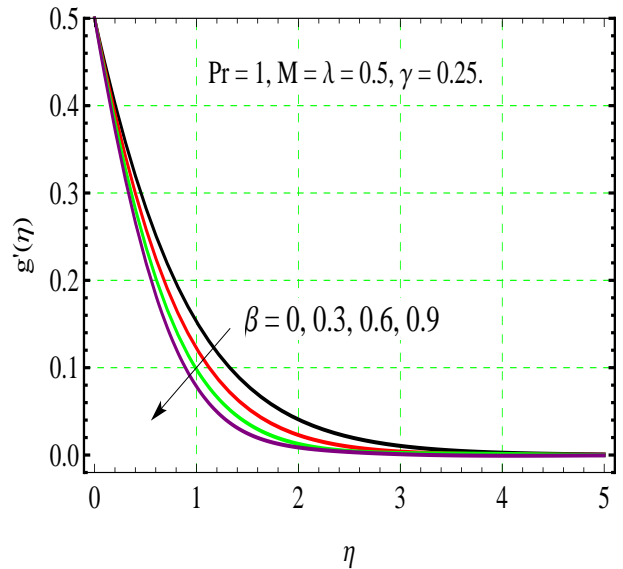


Fig. 3.3 – Effect of β on $g'(\eta)$.

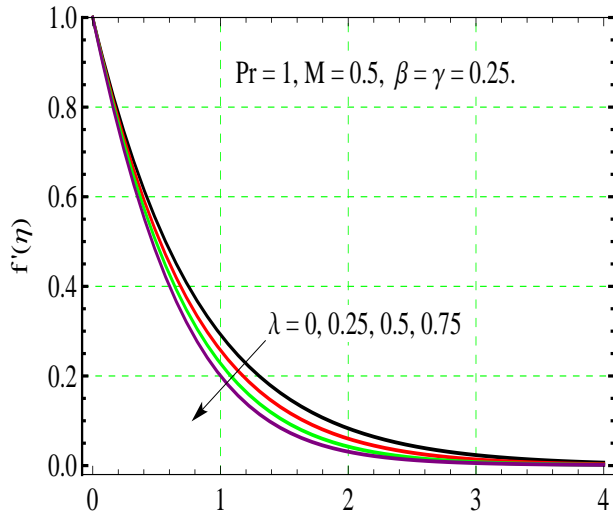


Fig. 3.4 – Effect of λ^η on $f'(\eta)$.

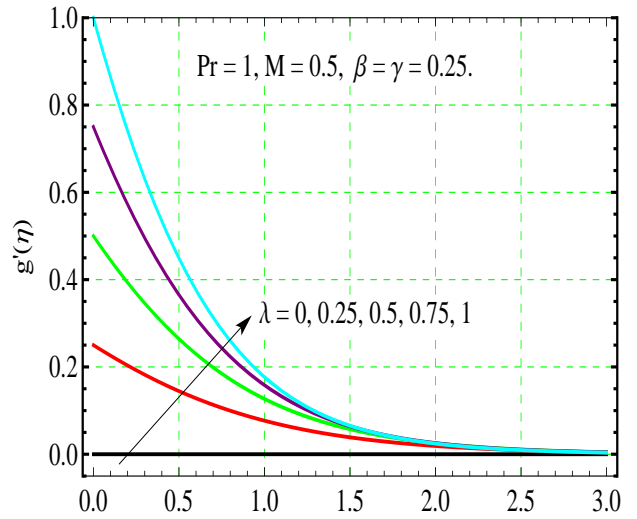


Fig. 3.5 – Effect of λ^η on $g'(\eta)$.

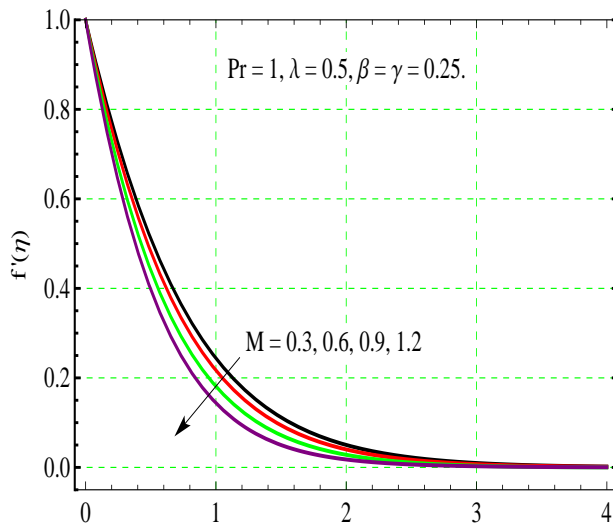


Fig. 3.6 – Effect of M^η on $f'(\eta)$.

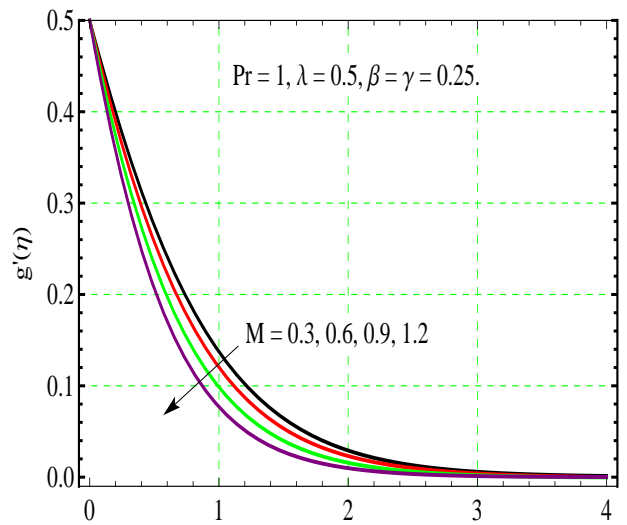


Fig. 3.7 – Effect of M^η on $g'(\eta)$.

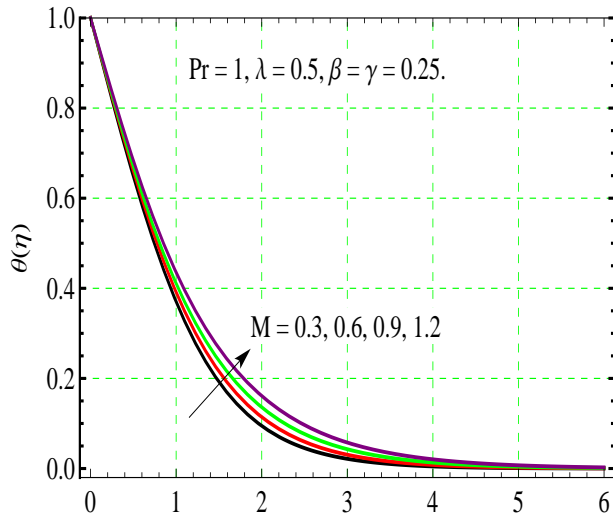


Fig. 3.8 – Effect of M on $\theta(\eta)$.

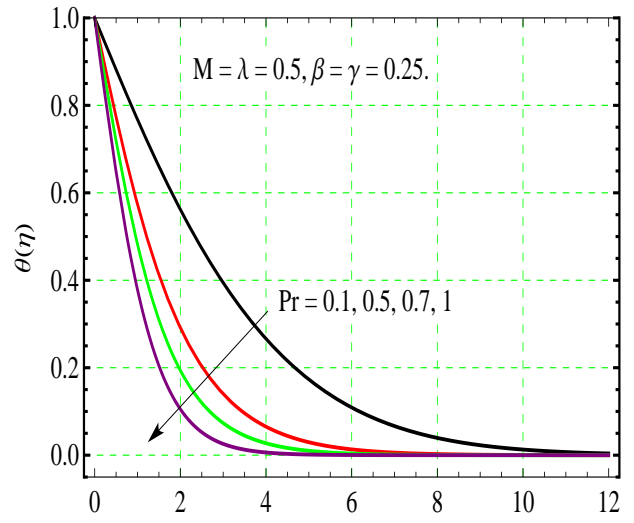


Fig. 3.9 – Effect of Pr on $\theta(\eta)$.

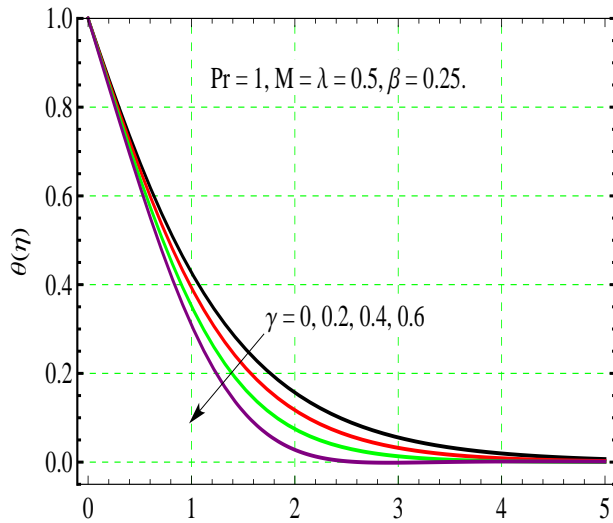


Fig. 3.10 – Effect of γ on $\theta(\eta)$.

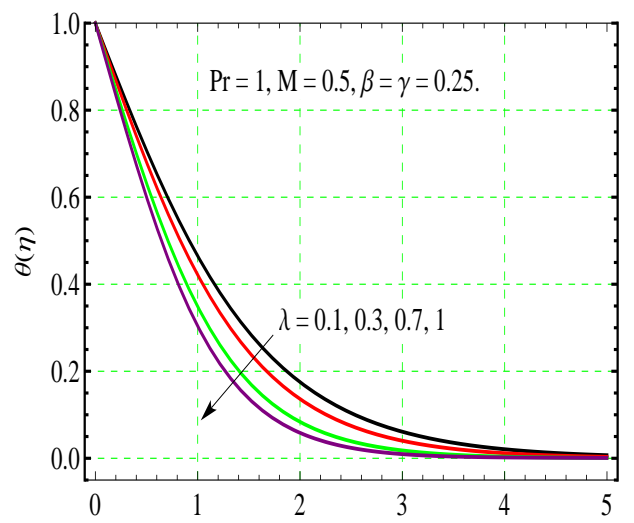


Fig. 3.11 – Effect of λ on $\theta(\eta)$.

β	γ	M	$\theta'(0)$
0	0.25	0.5	-0.75689
0.2			-0.72298
0.4			-0.69171
0.6			-0.66313
0.25	0		-0.67657
	0.2		-0.70680
	0.4		-0.74072
	0.6		-0.77877
	0.25	0	-0.74203
		0.5	-0.71491
		1	-0.64859

Table 3.2 – Values of wall temperature gradient $\theta'(0)$ for different value of β, γ, M when $h = -0.8$ $Pr = 1$ and $\lambda = 0.5$.

Chapter 4

Conclusions

This thesis deals with analytic solutions for flow and heat/mass transfer problem involving upper-convected Maxwell (UCM) fluid. Heat transfer through recently proposed Cattaneo-Christov model is considered. The following are the main observation of this study.

- In homotopy analysis method (HAM), there is freedom to choose initial guess and linear operator.
- Convergence of the obtained homotopy solution is ensured by choosing the suitable value of the convergence control parameter \hbar .
- The velocity and boundary layer thickness are decreasing functions of the fluid relaxation time λ_1 .
- The velocity gradients $f''(0)$ and $g''(0)$ are found to increase upon increasing the fluid relaxation time λ_1 .
- The concentration field ϕ decreases when Sc increases.
- The concentration field ϕ has opposite results for destructive $\gamma > 0$ and generative $\gamma < 0$ chemical reactions.

- Hartman number M supports the thickness of thermal boundary layer.
- Temperature and thermal boundary layer have inverse relationship with relaxation time for heat flux λ_2 .
- The present model reduces to the case of Newtonian fluid by choosing $\beta = 0$.

Bibliography

- [1] J. B. J. Fourier, *Théorie Analytique De La Chaleur*, Paris, 1822.
- [2] C. Cattaneo, Sulla conduzionedelcalore, *AttiSemin. Mat. Fis. Univ. Modena Reggio Emilia* 3 (1948) 83-101.
- [3] C. I. Christov, On frame indifferent formulation of the Maxwell-Cattaneo model of finite-speed heat conduction, *Mech. Res. Commun.* 36 (2009) 481-486.
- [4] B. Straughan, Thermal convection with the Cattaneo-Christov model, *Int. J. Heat Mass Transf.* 53 (2010) 95-98.
- [5] M. Ciarletta and B. Straughan, Uniqueness and structural stability for the Cattaneo-Christov equations, *Mech. Res. Commun.* 37 (2010) 445-447.
- [6] V. Tibullo and V. Zampoli, A uniqueness result for the Cattaneo-Christov heat conduction model applied to incompressible fluids, *Mech. Res. Commun.* 38 (2011) 77-79.
- [7] S. Han, L. Zheng, C. Li and X. Zhang, Coupled flow and heat transfer in viscoelastic fluid with Cattaneo-Christov heat flux model, *Appl. Math. Lett.* 38 (2014) 87-93.
- [8] M. Mustafa, Cattaneo-Christov heat flux model for rotating flow and heat transfer of upper-convected Maxwell fluid, *AIP Adv.* 5 (2015) doi: 10.1063/1.4917306.

- [9] J. A. Khan, M. Mustafa, T. Hayat and A. Alsaedi, Numerical Study of Cattaneo-Christov heat flux model for viscoelastic flow due to an exponentially stretching surface, *PloS one* 10 (2015) doi: 10.1371/journal.pone.0137363.
- [10] T. Hayat, M. Imtiaz, A. Alsaedi and S. Almezal, On Cattaneo-Christov heat flux in MHD flow of Oldroyd-B fluid with homogeneous-heterogeneous reactions, *J. Magn. Magn. Mater.* 401 (2016) 296-303.
- [11] L. Zheng, J. Niu, X. Zhang and Y. Gao, MHD flow and heat transfer over a porous shrinking surface with velocity slip and temperature jump, *Mathe. Comp. Model.* 56 (2012) 133-144.
- [12] R. Dhanai, P. Rana and L. Kumar, MHD mixed convection nanofluid flow and heat transfer over an inclined cylinder due to velocity and thermal slip effects: Buongiorno's model, *Pow. Tech.* In press (2015) doi:10.1016/j.powtec.2014.11.004.
- [13] F. Mabood, W. A. Khan and A. I. M. Ismail, MHD boundary layer flow and heat transfer of nano fluids over a nonlinear stretching sheet: A numerical study, *J. Magn. Magn. Mater.* 374 (2015) 569-576
- [14] A. K. Abdul Hakeem, N. Vishnu Ganesh and B. Ganga, Magnetic field effect on second order slip flow of nanofluid over a stretching/shrinking sheet with thermal radiation effect, *J. Magn. Magn. Mater.* 381 (2015) 243-257.
- [15] M. M. Rashidi, M. Nasiri, M. Khezerloo and N. Laraqi, Numerical investigation of magnetic field effect on mixed convection heat transfer of nanofluid in a channel with sinusoidal walls, *J. Magn. Magn. Mater.* 401 (2016) 159-168.
- [16] T. Hayat, S. Bibi, M. Rafiq, A. Alsaedi and F. M. Abbasi, Effect of an inclined magnetic field on peristaltic flow of williamson fluid in an inclined chan-

- nel with convective conditions, *J. Magn. Magn. Mater.* In press (2015) doi: 10.1016/j.mmm.2015.10.107.
- [17] T. Hayat, Z. Nisar, B. Ahmad and H. Yasmin, Simultaneous effects of slip and wall properties on MHD peristaltic motion of nanofluid with Joule heating, *J. Magn. Magn. Mater.* 395 (2015) 48-58.
- [18] C. Fetecau, M. Jamil, C. Fetecau and I. Siddiqui, A note on the second problem of Stokes for Maxwell fluids, *Int. J. Non-Linear Mech.* 44 (2009) 1085-1090.
- [19] M. Kumari and G. Nath, Steady mixed convection stagnation-point flow of upper convected Maxwell fluids with magnetic field, *Int. J. Non-Linear Mech.* 44 (2009) 1048-1055.
- [20] T. Hayat, M. Mustafa and S. Mesloub, Mixed convection boundary layer flow over a stretching surface filled with a Maxwell fluid in presence of Soret and Dufour effects, *Z. Naturforsch.* 65a (2010) 401-410.
- [21] K. L. Hsiao, MHD mixed convection for viscoelastic fluid past a porous wedge, *Int. J. Non-Linear Mech.* 46 (2011) 1-8.
- [22] S. Karra, V. Prusa and K. R. Rajagopal, On Maxwell fluids with relaxation time and viscosity depending on the pressure, *Int. J. Non-Linear Mech.* 46 (2011) 819-827.
- [23] T. Hayat, M. Mustafa, S. A. Shehzad and S. Obaidat, Melting heat transfer in the stagnation-point flow of an upper-convected Maxwell (UCM) fluid past a stretching sheet, *Int. J. Numer. Meth. Fluids* 68 (2012) 233-243.
- [24] S. Shateyi, A new numerical approach to MHD flow of a Maxwell fluid past a vertical stretching sheet in the presence of thermophoresis and chemical reaction, *Bound. Val. Prob.* 196 (2013) doi: 10.1186/1687-2770-2013-196.

- [25] K. L. Hsiao, Conjugate heat transfer for mixed convection and Maxwell fluid on a stagnation point, Arab. J. Sci. Eng. 39 (2014) 4325-4332.
- [26] A. Mushtaq, M. Mustafa, T. Hayat and A. Alsaedi, Effect of thermal radiation on the stagnation-point flow of upper-convected Maxwell fluid over a stretching sheet, J. Aerosp. Engg. 27 (2014) 04014015.
- [27] M. Mustafa, J. A. Khan, T. Hayat and A. Alsaedi, Sakiadis flow of Maxwell fluid considering magnetic field and convective boundary conditions, 5 (2015) doi: 10.1063/1.4907927.
- [28] T. Hayat, Z. Abbas and M. Sajid, Series solution for an upper-convected Maxwell (UCM) fluid over a porous stretching plate, Phys Lett. A 358 (2006) 396403.
- [29] T. Hayat, Z. Abbas and M. Sajid, MHD boundary layer flow of an upper-convected Maxwell (UCM) fluid in a porous channel, Theor. Comput. Fluid Dyn. 20 (2006) 229238.
- [30] T. Hayat and M. Sajid, Homotopy analysis of MHD boundary layer flow of an upper-convected Maxwell (UCM) fluid, Int. J. Eng. Sci. 45 (2007) 393401.
- [31] V. Aliakbar, A. A. Pahlavan and K. Sadeghy, The influence of thermal radiation on MHD flow of Maxwellian fluids above stretching sheets, Comm. Nonlinear Sci. Num. Simu. 14 (2009) 779794.
- [32] A. A. Pahlavan, V. Aliakbar, F. V. Farahani and K. Sadeghy, MHD flows of UCM fluids above porous stretching sheets using two-auxiliary-parameter homotopy analysis method, Comm. Nonlinear Sci. Numer. Simulat. 14 (2009) 473488.

- [33] A. A. Pahlavan and K. Sadeghy, On the use of homotopy analysis method for solving unsteady MHD flow of Maxwellian fluids above impulsively stretching sheets, *Comm. Nonlinear Sci. Num. Simu.* 14 (2009) 13551365.
- [34] T. Hayat, Z. Abbas and N. Ali, MHD flow and mass transfer of a upper-convected Maxwell fluid past a porous shrinking sheet with chemical reaction species, *Phys. Lett. A* 372 (2008) 46984704.
- [35] T. Hayat and Z. Abbas, Channel flow of a Maxwell fluid with chemical reaction, *Z. Angew. Math. Phys.* 59 (2008) 124144.
- [36] T. Hayat, Z. Abbas and M. Sajid, MHD stagnation-point flow of an upper-convected Maxwell fluid over a stretching surface, *Chaos, Solitons and Fractals* 39 (2009) 840848.
- [37] S. J. Liao, On the homotopy analysis method for nonlinear problems, *Appl. Math. comput.* 147 (2004) 499-513.
- [38] T. Hayat, M. Awais, M. Qasim and A. A. Hendi, Effects of mass transfer on the stagnation point flow of an upper-convected Maxwell (UCM) fluid, *Int. J. Heat Mass Transf.* 54 (2011) 3777-3782.